Magnetic-field penetration and structure of the mixed state in a superconductor with a multicomponent order parameter

A. S. Zeltser, Yu. G. Pashkevich, and A. E. Filippov
A. A. Galkin, Donetsk Phystech of National Academy of Sciences of Ukraine, 83114 Donetsk, Ukraine
(Received 26 April 1999; revised manuscript received 5 April 2000)

Magnetic-field penetration in superconductors with a multicomponent order parameter is discussed. Numerical simulation of the process is performed for a wide range of the external magnetic field and internal parameters of the system. It is found that the kinetic process of the vortex penetration regularly produces domain boundaries separating phases with different realizations of the equilibrium order parameter. As a result a new (mixed) vortex state can appear. It contains two different types of vortices connected to pairs and chains by the surface domain energy. The lattice formed by such vortices has a symmetry lower than hexagonal or tetragonal ones.

I. INTRODUCTION

The nontrivial localized structures in superconductors with multicomponent pairing as well as superfluid ^{3}He have been actively studied recently. The ordering kinetics and topology of nonlinear excitations in these systems have many common features.[1–6] In particular, the multicomponent nature and anisotropy produces a solitary vortex of complicated structure[7–11] and modifies the interaction between vortices.[12,13,6]

The multicomponent nature of the order parameter in such systems leads to phase domains with equivalent energies and different equilibrium realizations of the order parameter components. Within the domain boundaries the order parameter has a complicated (lower) symmetry with all components nonzero. It favors the generation of vortex excitations inside the domain boundaries.[6] These properties were predicted[1] and reproduced recently for the ordering kinetics in numerical experiments.[3,4,6]

Vortices with a magnetic flux appearing at intermediate stages of the kinetic scenario are anisotropic. The anisotropy can be generated by the crystal lattice anisotropy (in this case it is reflected in rhombic terms in the gradient part of the free energy functional[8–10]) as well as being due to the multicomponent nature of the order parameter by itself.[8,6]

A more complicated picture appears in the presence of an external magnetic field. It was predicted from semianalytical estimations that a different equilibrium configuration of the order parameter zeros can generate different vortex lattices and produce phase transitions between these structures.[14] In turn, the vortex anisotropy lowers the symmetry of the vortex lattice down to a rhombic lattice.[12,13] All recent theoretical studies predict some deviations of the vortex lattice from the traditional triangular lattice.[15–19]

The deviation of the vortex lattice from the traditional one is caused by the competition between the magnetic field and the effect of anisotropy. It takes place when the energy of the anisotropy is comparable to the magnetic energy. In this case the variation of the order parameter and the magnetic field vector potential has to be accounted for self-consistently in a frame of numerical simulation. In the present study we show that the above competition between energies can lead to new nontrivial vortex structures in these systems.

The goal of this paper is to present the results of a numerical simulation of the magnetic-field penetration into superconductors with anisotropic pairing. The simulation is based on the time-dependent Ginzburg-Landau model (TDGLM). This model self-consistently takes into account all components of the order parameter and the magnetic-field vector potential. These equations give a rigorous description of the system given the appropriate initial and boundary conditions.[6,20]

In particular, when the magnetic field penetrates into a uniformly ordered superconducting system the TDGLM allows one to describe carefully both the kinetics of the penetration process and the resultant stationary structure.[21–24] It should be noted that some of these structures found do not coincide with a simple picture predicted from naive mean-field estimations. Sometimes the final distribution of the vortices can be even the nonequilibrium state. Thus, it represents a memory about ''frozen'' kinetics. Nevertheless, this structure is determined by the penetration process, which normally appears in kinetics, and as such it must be treated as a physical state and expected to be observed.[25–27]

Experimental information about real systems can be obtained from positions and structure (form factor) of the maxima of the correlation function which is observed in small-angle neutron scattering (SANS) experiments on a vortex lattice.[28–32]

II. TIME-DEPENDENT GINZBURG-LANDAU MODEL

A. Free energy

We apply the standard Ginsburg-Landau free energy functional expanded over order parameter variables $\eta = [\eta_x, \eta_y]$:

$$F = \frac{1}{2}\int d^d r \Big\{ a\,\eta\eta^* + \frac{\beta_1}{2}(\eta\eta^*)^2 + \frac{\beta_2}{2}|\eta\cdot\eta|^2 + \beta_3(|\eta_x|^4 + |\eta_y|^4) + K_1 D_i^* \eta_j^* D_i \eta_j + K_2 D_i^* \eta_i^* D_j \eta_j + K_3 D_i^* \eta_j^* D_j \eta_i + K_z D_z^* \eta_j^* D_z \eta_j + \gamma(\nabla\times\mathbf{A})^2 \Big\}. \quad (1)$$

These variables appear from an expansion of the aniso-

 ©2000 The American Physical Society

tropic superconducting gap $\Delta(\mathbf{k})$ over functions $\Phi_j(\mathbf{k})$ belonging to one of the irreducible representations of the crystal point group $\Delta(\mathbf{k})=\Sigma\,\eta_j\Phi_j(\mathbf{k})$. This expansion creates a vector order parameter with complex coefficients $\eta_x=\eta_1+i\,\eta_2$ and $\eta_y=\eta_3+i\,\eta_4$. Here, the following notation is used: $a=\alpha(T-T_c)$, $D_i=\partial_i-i\ gA_i$, $j=x,y$; $\gamma=1/8\pi$, $g=e/\pi hc$; and $\mathbf{A}=(A_x,A_y)$ is the vector potential.

Specific properties of particular systems are associated with the phenomenological constants $\alpha,\beta_1,\beta_2,\beta_3$, and K_j. The free energy functional and TDGLM equations can be derived from microscopics.[5,20] The corresponding phenomenological constants in the equations can be restored from the microscopic parameters of the system. However, from a phenomenological point of view only the magnetic stability

$$K_1+K_2+K_3>|K_3|,\quad K_1>|K_2|,\quad K_4>0$$

and positiveness of quadratic form

$$\beta_1+\beta_2+\frac{\beta_3}{2}+\min\left\{\frac{\beta_3}{2},-\frac{\beta_2+|\beta_2|}{2}\right\}>0,$$

restrict these constants.

B. TDGLM equations, and initial and boundary conditions

A set of coupled equations for the TDGLM has been derived[20] for the general case of superconductors of mixed *d* and *s* symmetry from the Gor'kov equations. It was applied, in particular, to study the structure of a solitary vortex in a superconductor with anisotropic pairing.[11,10] Here we use the following representation for the TDGLM equations:

$$\frac{\partial\eta_j}{\partial t}=-\Gamma\frac{\delta F}{\delta\eta_j}+\xi_j(\mathbf{r},t),$$

$$\frac{\partial\mathbf{A}}{\partial t}=-\Gamma_A\frac{\delta F}{\delta\mathbf{A}}+\xi_A(\mathbf{r},t),\qquad(2)$$

where Γ and Γ_A are positive relaxation constants. Equations (2) describe the evolution of the order parameter components η_j at the only *d*-wave pairing symmetry. Some additional freedom comes here from the inclusion of random fluctuations. All fields of the problem are supposed to fluctuate independently with Gaussian correlators $\langle\xi_j(\mathbf{r},t)\rangle=0$ and $\langle\xi_j(\mathbf{r},t)\xi_k(\mathbf{r}',t)\rangle=\delta_{jk}\delta(\mathbf{r}-\mathbf{r}')\,\delta(t-t')$.

To study field penetration we solve Eqs. (2) at fixed initial conditions. These conditions correspond to one of the uniformly ordered states. The possible states are determined by the given relations between the phenomenological constants. It is convenient to classify these states using the following cyclic variables: $\eta_y^*\eta_x=L-iM$ and $\eta_x^*\eta_y=L+iM$, where

$$M=(\eta_x^*\eta_y-\eta_y^*\eta_x)/2i=i\mathbf{e}_z(\eta\times\eta^*)/2=[\eta_1\eta_4-\eta_2\eta_3],$$

$$L=(\eta_x^*\eta_y+\eta_y^*\eta_x)/2=[\eta_1\eta_3+\eta_2\eta_4].$$

Introducing the order parameter density $\mathbf{S}=(S_1,S_2,S_3)$ and the superconducting current $\mathbf{J}$,

$$S=\eta\eta^*=|\eta_x|^2+|\eta_y|^2,$$

$$S_1=P=|\eta_x|^2-|\eta_y|^2,\quad S_2=2M,\quad S_3=2L,$$

$$\mathbf{J}=\eta_1\nabla\eta_2-\eta_2\nabla\eta_1+\eta_3\nabla\eta_4-\eta_4\nabla\eta_3-\mathbf{A}|S|,$$

one can rewrite the free energy functional, Eq. (1), in a more convenient form:

$$F[\mathbf{S},\mathbf{J}]=\frac{1}{2}\int d^dr\left\{\left[\frac{1}{4}\Sigma_j(\nabla S_j)^2+J^2\right]\Big/\,|S|-|S|+\frac{1}{2}S^2-\frac{1}{4}b_2S_2^2-\frac{1}{4}b_3S_3^2+\gamma(\nabla\times\mathbf{A})^2\right\}.\qquad(3)$$

This functional generates a relatively compact system of TDGLM equations,

$$\frac{\partial\eta_j}{\partial t}=\Delta\eta_j-(-1)^j(2\mathbf{A}\cdot\nabla\eta_k+\eta_k\nabla\mathbf{A})-\eta_j[A^2-1+S]+b_2M\frac{\partial M}{\partial\eta_j}+b_3L\frac{\partial L}{\partial\eta_j}+\xi_j(\mathbf{r},t),$$

$$\frac{\partial\mathbf{A}}{\partial t}=\theta_A\{-\nabla\times(\nabla\times\mathbf{A})+\frac{1}{\kappa^2}[(\eta_1\nabla\eta_2-\eta_2\nabla\eta_1)+(\eta_3\nabla\eta_4-\eta_4\nabla\eta_3)-\mathbf{A}|S|]+\xi_A(\mathbf{r},t)\},\qquad(4)$$

which can be initially analyzed in terms of the reduced constants

$$b_2=\frac{2\beta_2+\beta_3}{\beta_1+\beta_2+\beta_3},$$

$$b_3=\frac{\beta_3}{\beta_1+\beta_2+\beta_3}$$

before numerical simulation. Here and below we use the following reduced variables:

$$\eta_j=\eta_j\sqrt{\frac{\beta_1+\beta_2+\beta_3}{a}},$$

$$\theta_A=\frac{\Gamma_A}{8\pi\alpha\xi^2\Gamma},\quad \xi=\sqrt{\frac{K_1}{a}}$$

as in previous articles.[6] We suppose that the Ginzburg-Landau parameter $\kappa\gg1$ (as it is for novel superconductors). Besides, we limit ourselves by the approximation of small square anisotropy $|K_2|$, $|K_3|\ll|K_1|$ used in previous studies.[5,6] As seen from Eq. (3), at $|K_2|$, $|K_3|\ll|K_1|$ the symmetry of the equilibrium uniform structure is completely determined by the factors $b_{2,3}$ at the invariants *M* and *L*, respectively.

Simple analysis gives the possible uniform structures classified in Ref. 6. It is shown in Ref. 6 that some symmetry transformations perform mutual permutations of the physically equivalent phases. Due to this, we can restrict further numerical simulations by one of the phases (simplest for an analysis and graphic presentation of the results). It is seen from the structure of $F[\mathbf{S},\mathbf{J}]$ that the simplest configuration

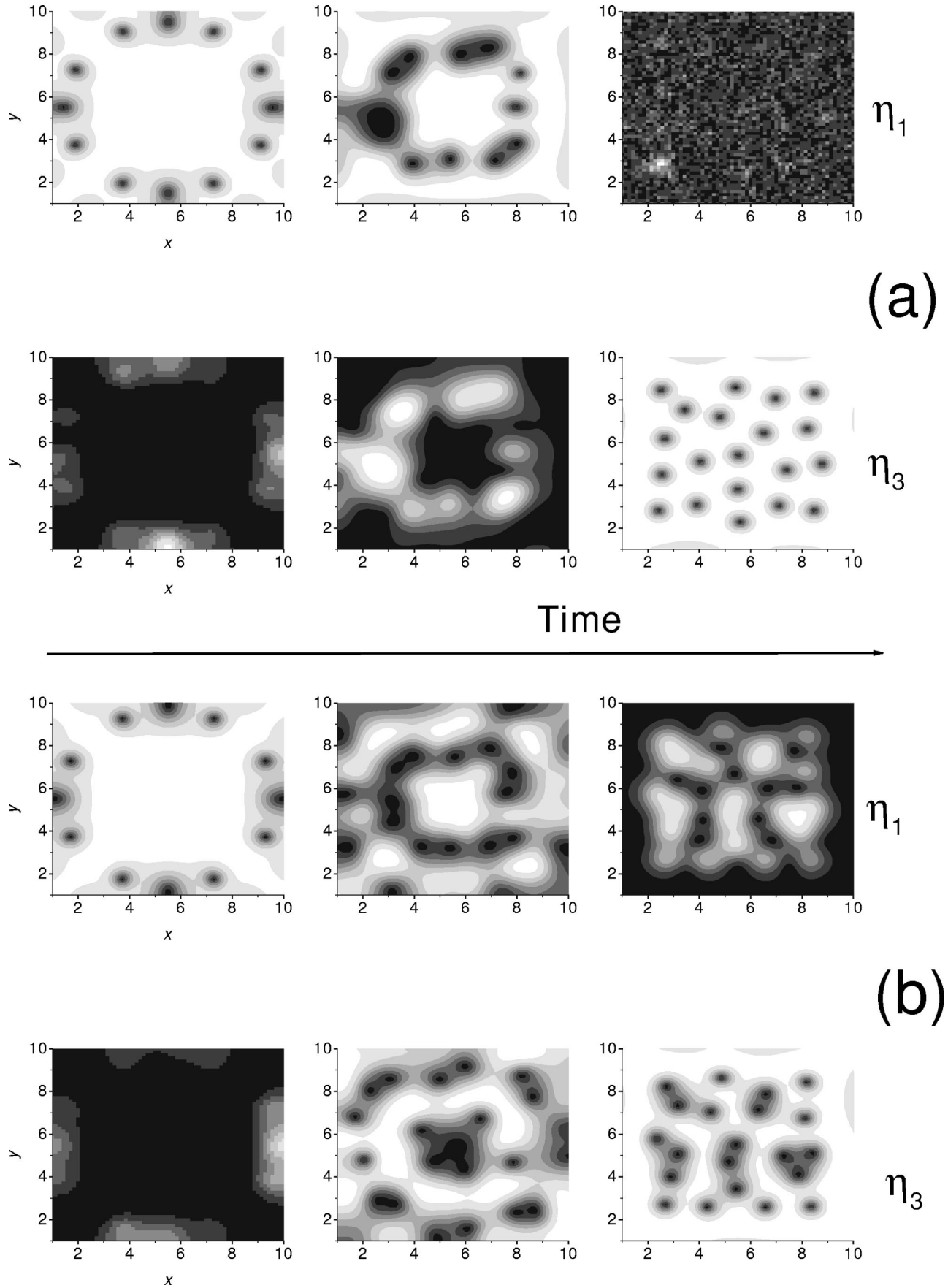

FIG. 1. Two typical kinetic scenarios of the penetration of a magnetic field which lead to the creation of two different final states in the phase diagram [$\eta_3 \neq 0, \eta_1 = 0$ in (a) and $\eta_{3,1} \neq 0$ in (b), respectively]. The densities of the different components of the order parameter are shown by gray-scale maps normalized to the difference between the maximum and minimum of each ordering field. The initial state ($\eta_1 = 1, \eta_{2,3,4} = 0$) is the same for both (a) and (b) cases. The pictures at the left side correspond to some initial but already nonzero time.

appears in equilibrium when $L \to 0$ and $M \to 0$ at $b_3 < 0$ and $b_2 < 0$ (it corresponds to phase II in Ref. 6). In this phase two kinds of equilibrium domains are possible. The equilibrium values of the order parameter $\eta = [\eta_x, \eta_y]$ in the domains are given by the relations $\eta = [\eta_x, 0]$, where $\eta_x \neq 0$ and $\eta = [0, \eta_y]$, $\eta_y \neq 0$, respectively. At the same time the values M and L are not equal to zero only inside the domain walls. So, as the initial condition for a uniform state one can take simply $|\eta_x| = \eta_1 = 1, \eta_{2,3,4} = 0$ (or alternatively $|\eta_y| = \eta_3 = 1, \eta_{1,2,4} = 0$).

For definiteness (to reduce the number of possible combinations of the parameters) we restrict the present study by the subspace $b_3 = b_2 < 0$. This choice in particular can be supported by the results of a renormalization-group study of the problem.[6] This study shows that the effective renormalized parameters b_3 and b_2 are attracted to the vicinity of the line $b_3 = b_2$ in sector $b_3 < 0, b_2 < 0$. It corresponds to $\beta_2 \to 0$. Numerical simulations for other negative b_3 and $b_2 (\beta_2 \neq 0)$ give qualitatively the same results.

The boundary conditions for A are given by the requirement that the magnetic field at the external surfaces of the sample, $B = \nabla \times A$, must be equal to H_{ext}. Here the magnetic field is measured in units of the upper critical field $H_{c2} = \phi_0 / 2\pi\xi^2$ and the vector potential A in units of $H_{c2}\xi(0)$, respectively. Let us note also that we consider a two-dimensional problem, i.e., cylindrical geometry with a square cross section. This means that the sample is assumed to be infinite in the z direction and all derivatives along this direction can be neglected.[21,33,34] For definiteness all numerical procedures were done where the value of the Ginzburg-Landau parameter is chosen to be $\kappa = 20$; i.e., we consider a strongly pronounced type-II superconductor.

It was argued in Ref. 24 that the choice of boundary conditions of the order parameter has no strong effect on the growth of the superconducting structure provided the superconducting region is several coherence lengths away from the boundary. Accounting for this, the superconductor-vacuum interface is usually used to simulate the general properties of superconducting systems.[21–24,34] In this case the order parameter must satisfy the condition $(-i\nabla - A)\eta|_n = 0$, which assures zero current through the superconductor-vacuum interface.

At sufficiently high fields H_{ext}, the value of A at the boundary (which is proportional to the size of the system) can become very large, causing an instability of the numerical procedure. This difficulty is usually bypassed by using the so-called link variable approach: the order parameter is defined at the nodes of a rectangular mesh, while at the links, a link variable $U_\mu = \exp[-i\int A_\mu d\mu]$ is used, with $\mu = x$ or $\mu = y$ depending on the direction of the link. This approach was described in detail in different papers (see, e.g., Refs. 21–24). It can be directly extended to the system with anisotropic pairing, and we use it here for calculations without further modifications.

III. NUMERICAL SIMULATION

It was found that the phase diagram for the system with anisotropic pairing placed into an external magnetic field can be more complicated than was expected from treating the mean field. The main new feature is the possibility of a stable mixed state. In this state the superconducting order parameter $S = \eta\eta^* = |\eta_x|^2 + |\eta_y|^2$ has two sets of minima (vortices) with different magnitudes of the S density and, as a result, with different magnetic fluxes inside the vortices.

The results of numerical simulations are summarized in Figs. 1–5. Let us discuss first of all qualitatively the kinetic scenario and resulting structures expected. For this goal it is convenient to use the order parameter components $\eta_1, \ldots, \eta_4$ instead of the physically measured value of the magnetic flux. These components were used already for a mean-field description. In these terms the newly found mixed state contains two ordered components $\eta = [\eta_1, 0, \eta_3, 0]$ with different $\eta_1 \neq \eta_3$, but nonzero magnitudes (in contrast to the mean field predicting one ordered component in sector $b_3 < 0$ and $b_2 < 0$).

The mean-field approximation is valid for a uniformly ordered system only. Penetration of the magnetic field produces a nonuniform distribution of the order parameter. Especially it is essential in the vicinity of the vortices where the magnitude of one of the components of the order parameter turns to zero. In this region the nonzero value for another component (which was suppressed in the uniform state) is found to be more preferable. It grows and suppresses other fields of the problem in some neighborhood. Below we concentrate on kinetic scenarios for the particular initial conditions $\eta_1 \neq 0, \eta_{2,3,4} = 0$.

Two typical kinetic scenarios of the field penetration of the magnetic field for two different states in a phase diagram are presented in Figs. 1(a) and 1(b), respectively. The densities are shown by gray-scale maps normalized at every time moment into a difference between the maximum and minimum of each ordering field. The first scenario [shown in Fig. 1(a)] takes place for big values of the phenomenological constants $b_{2,3}$. It leads to the final state in which only one component of the field (η_3) is ordered. In the second case both fields coexist in the final state. These two states have a different topology of the physically observable vortex state.

To make the pictures detailed we present here the structures appearing in small numerical boxes having 64×64 calculation cells [with the size of the cell corresponding to a physical length equal to $\xi(0)/2$]. These calculations were tested numerically for different *system sizes* (from 128×128 up to 512×512 unit cells in a square geometry) as well as for a *rectangular* cross section (with 128×256 numerical cells). All these simulations lead to the same topology of the vortex structures and to very close quantitative results for the averaged parameters used below for the numerical identification of the states.

A small magnetic field does not produce any vortex in the system. So if we are probing the field range below the lower critical field, the trial order parameter $\eta_1 \neq 0$ is slightly suppressed by the field only in the vicinity of the boundary. At a higher field some magnetic flux goes inside the system in the form of vortices.

As is seen from Figs. 1(a) and 1(b), an initial process of field penetration into the system is qualitatively the same in both phases. One can note the usual cylindrical vortices penetrating across the planar boundaries and avoiding the angles of the square. It coincides, as a matter of fact, with the same picture for a traditional superconductor with ordinary pairing.[21–23]

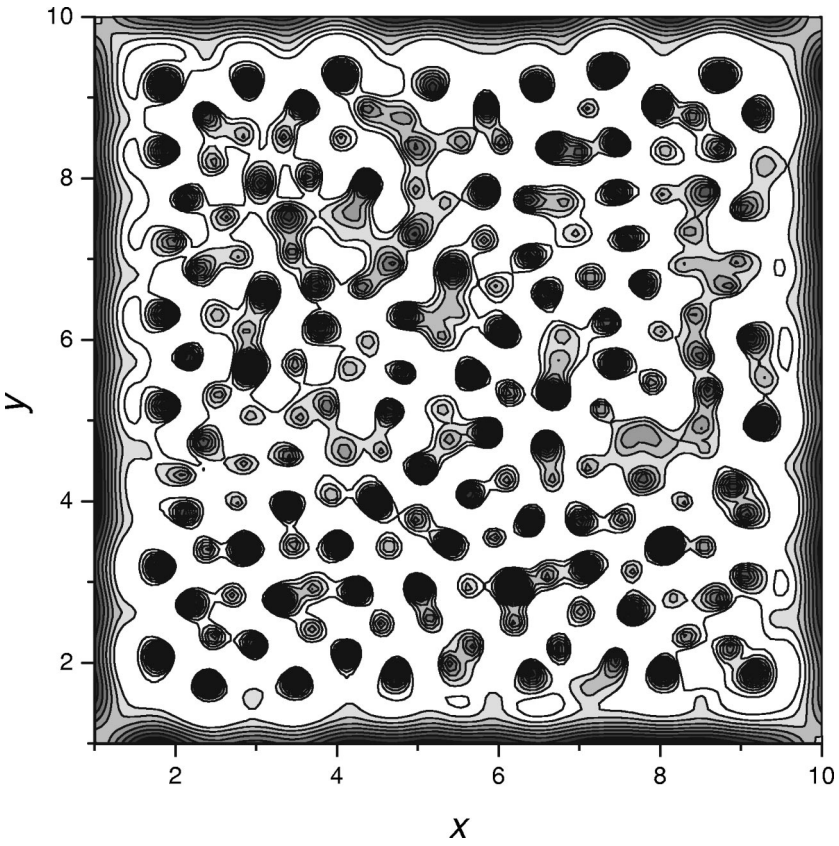

FIG. 2. Typical intermediate stage of the kinetic scenario containing solitary vortex pairs as well as some fragments of the chains. The distribution of the order parameter is shown by the gray-scale map accompanied by the contour lines.

The difference appears in an intermediate stage of the process. The magnetic flux inside the system causes a strong reconstruction of the state. It suppresses the initially ordered field η_1 and produces islands of a growing second field η_3. The inequality $\eta_1 > \eta_3$ transforms into the inverse relation $\eta_1 < \eta_3$.

The main distinction between the two scenarios (a) and (b) is directly visible from this step of the process. For big values of the phenomenological constants $b_{2,3}$, the impact to the energy from islands of the new state with $\eta_3 \neq 0$ is found to be so strong as to suppress another field $\eta_1 \neq 0$ completely. In the other case both fields coexist in the final state, but the inverse inequality $\eta_1 < \eta_3$ conserves. It is expected (and seen directly from the figures and numerical data) that these two states have a different topology of the vortex state. A direct relation exists between the coexistence of the fields $\eta_{1,3} \neq 0$ and the vortex flux structure. It was found that to describe quantitatively the phase diagram plotted in the $(b_{2,3};H)$ space, it is enough to calculate the order parameters $\langle \eta_1 \rangle$ and $\langle \eta_3 \rangle$ averaged over the system.[35]

For a strong magnetic field many vortices go inside the system. It suppresses both ordered fields in average. At a very high external field a state with a so-called ''surface superconductivity'' appears.[21–23] In this state both components of the order parameter are strongly suppressed inside the system. As a result, the impact from anisotropy [caused from the quartic terms $-\frac{1}{4}b_2 S_2^2 - \frac{1}{4}b_3 S_3^2$ in the functional (3)] becomes negligible in comparison with the magnetic-field energy (which is balanced by the second-order terms $[\frac{1}{4}\Sigma_j(\nabla S_j)^2 + J^2]/|S| - |S|$ in the free energy). In this state the magnetic field strongly dominates over the anisotropy at all values of the parameters $b_{2,3}$ and the resulting configuration coincides with the same for traditional superconductors with ordinary pairing.

IV. RESULTS AND DISCUSSION

The purpose of this study is to account for the competition between the magnetic field and the effect of the anisotropy to plot a phase diagram in the space $(b_{2,3},H)$ which compares the impacts from the corresponding energies.

It is seen from Fig. 1(a) that at some (quite big) phenomenological constants $b_{2,3}$ the islands of a new ordered field completely overcome the old field η_1. The resulting structure has only one ordered field η_3. The magnetic flux here is locked into the standard vortex lattice. It was proved by the simulation (for quite large volumes of the system, when the effect of the boundaries becomes negligible) that it tends to a regular hexagonal symmetry which is well known for traditional superconductors. In fact, in spite of the intermediate kinetics, this phase coincides with the mean-field prediction.[5,6]

Let us concentrate now on the second scenario. In this case the nonlocal energy (caused by the magnetic field and the surface tension of the vortices) prevails over the local anisotropy impact. The islands of the new ordered field η_3 cannot suppress the old one completely. In the final state two components of the order parameters coexist. Both fields hold the vortices containing the magnetic flux. Due to mutual repulsion, these vortices tend to form a hexagonal lattice. However, the magnitudes of the fields η_2 and η_3 are different. The vortices are different, too. It produces a specific instability in the vortex lattice. The vortices of two different kinds form the pairs.

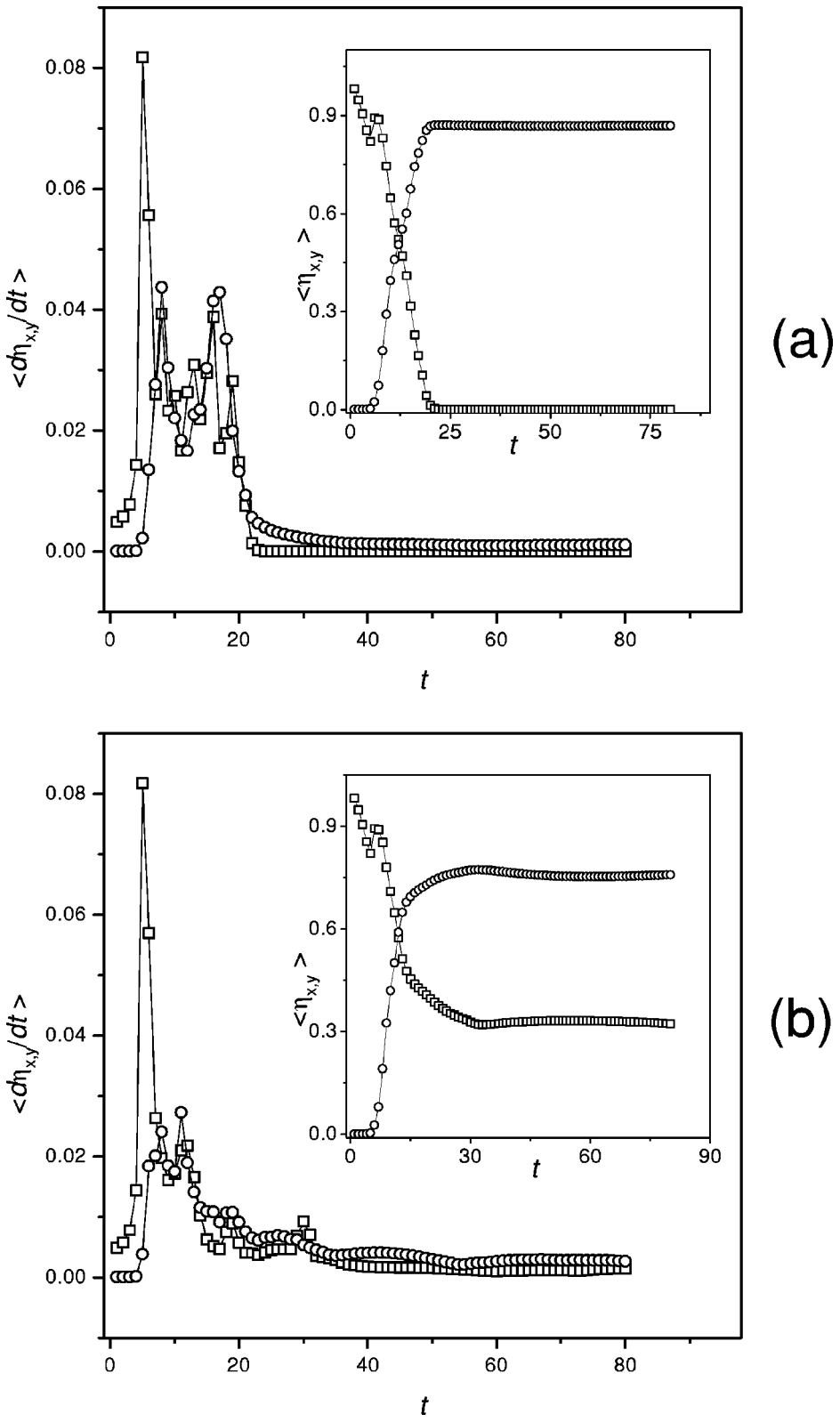

FIG. 3. Time dependences of the averaged time derivatives $\langle \partial \eta_1 / \partial t \rangle$ and $\langle \partial \eta_3 / \partial t \rangle$ corresponding to the kinetic scenarios (a) and (b) shown in Fig. 1. The time dependences of the averaged order parameter components $\langle \eta_1 \rangle$ and $\langle \eta_3 \rangle$. Here and further squares and circles are connected to η_1 and η_3 parameters, respectively.

These are not the usual vortex-antivortex pairs. The vortices of both kinds have the same direction of magnetic flux. This structure is obtained in the frame of self-consistent numerical simulation and in this sense it can be treated as a result of numerical experiment. However, it is interesting to discuss briefly a qualitative reason for this structure.

The averaged level of the magnetic field inside the system is determined by an integral flux of the vortices. But the vortices are different. The main repulsion between the vortices is already ''screened'' in a state close to the hexagonal lattice. So one can treat the distinction between the mean value of the field and magnetic fluxes of larger and smaller vortices as effectively ''positive'' and ''negative.'' These effective vortices are confined with two different kinds of real vortices and this causes a small attraction between them. This attraction is found numerically to be enough to produce

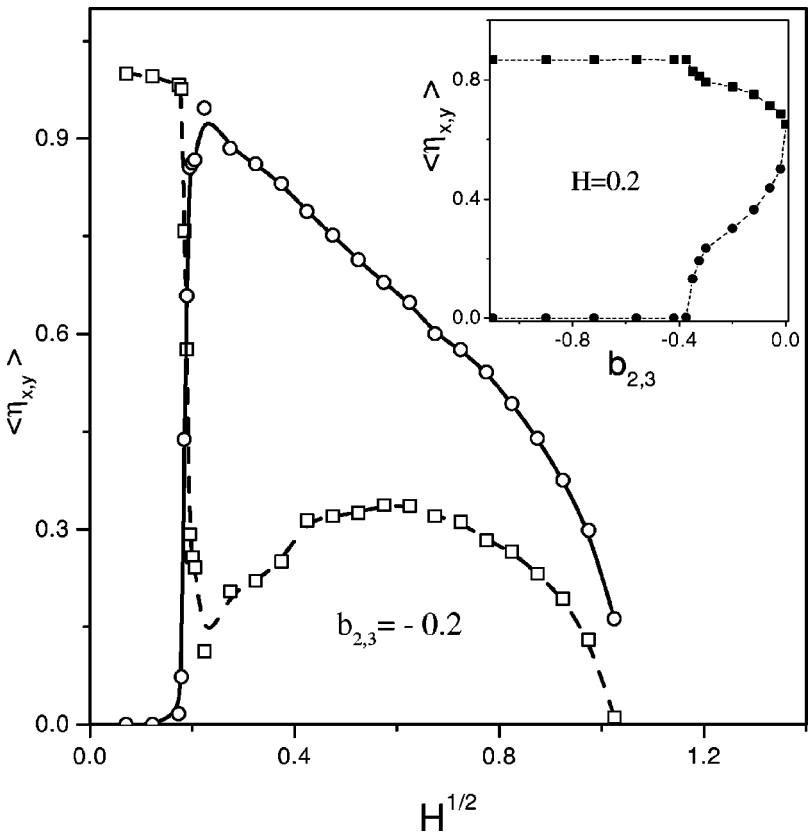

FIG. 4. Typical dependences of the averaged order parameter components $\langle \eta_1 \rangle$ and $\langle \eta_3 \rangle$ from the external magnetic field H at fixed values of the phenomenological constants. In the inset the dependences of the averaged order parameter components $\langle \eta_1 \rangle$ and $\langle \eta_3 \rangle$ from the values of phenomenological constants at fixed external magnetic field H are shown.

the above instability.

The screened vortices behave as effective ''Coulomb charges'' producing ''dipolar pairs.'' Further, these pairs interact as dipoles and form typical ''dipolar chains.''[36–39] It was found recently that such chains are attracting intermediate configurations for kinetic scenarios in different physical systems.[40] This stage exists for quite a long time (much longer than the previous stages) and in the presence of pinning it can be frozen as a stable (so-called ''virtual''[25–27]) phase. In the other case the ordering is continuous and the dipolar pairs orientate into parallel lines. A typical intermediate stage of the scenario described is presented in Fig. 2.

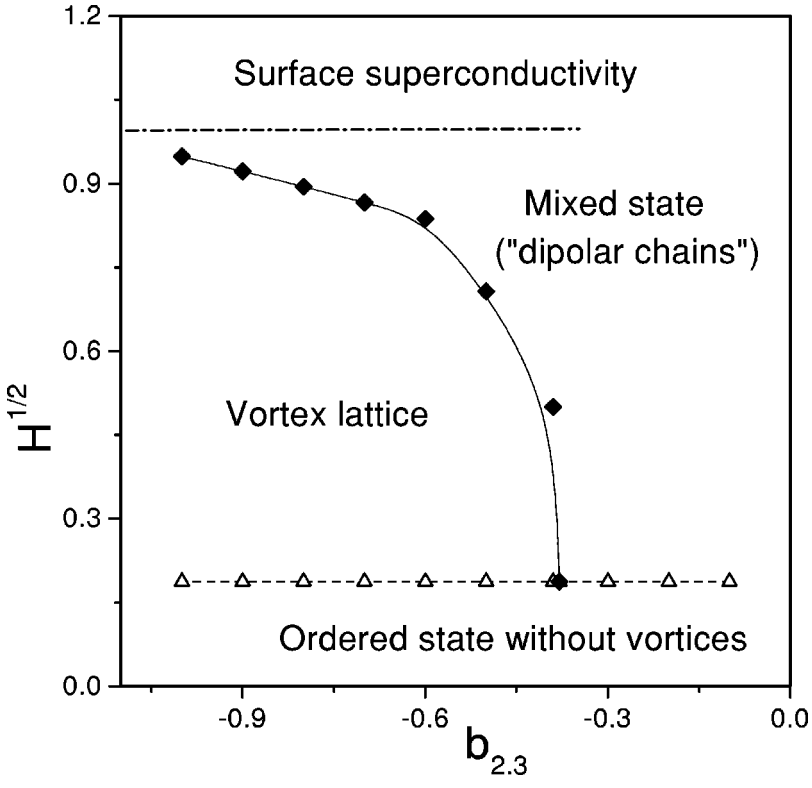

FIG. 5. Phase diagram in the space $(b_{2,3};H)$.

Here the distribution of the order parameter is shown by the gray-scale map accompanied by contour lines. Solitary vortex pairs as well as some fragments of the chains already presented in the system at the presented moment can be seen directly.

From a physical point of view it is the main *new feature of the system*. At some relation between parameters the superconductor with anisotropic pairing placed into an external magnetic field can form *two kinds of vortices* containing different magnetic fluxes. The flux associated with each vortex deviates from the standard flux quantum (and is not equal to two or more quanta).

This deviation exists in traditional superconductors also. It has been observed recently in a mesoscopic superconductor where the (small) total number of vortex cores allowed to enter the interior of the superconductor can be directly compared with discrete (but nonequidistant) energy levels.[41] In particular, it was found for a given number of vortices that the energy level is split due to different possible symmetries of the vortex configuration. It corresponds to a different total magnetic flux accumulated in the system with a noninteger number of magnetic flux quanta. In novel superconductors with anisotropic pairing this effect is accompanied (and, as is seen from numerical simulation, can be enforced) by the interaction between the components. It leads to the splitting between two kinds of vortices.

Let us define now integral parameters convenient to describe a phase diagram of the system numerically. One can note that after some transient process the averaged parameters $\langle \eta_{1,2} \rangle$ tend to stationary fixed values. Numerically this process of ordering of the fields $\eta_{1,2}$ can be controlled by the calculation of the averaged time derivatives $\langle \partial \eta_1 / \partial t \rangle$ and $\langle \partial \eta_3 / \partial t \rangle$ presented in Figs. 3(a) and 3(b), respectively.[35]

At the beginning of the curves the separate maxima of the derivatives are seen. These maxima correspond to a strong reordering of the system. It happens when first (one or two) layers of magnetic vortices penetrate simultaneously into the system across all symmetric boundaries. At later times of the process the magnetic flux in the system does not grow so quickly. This is reflected in the decrease of both derivatives $\langle \partial \eta_1 / \partial t \rangle$ and $\langle \partial \eta_3 / \partial t \rangle$. The time interval shown in the plots corresponds to 2×10^3 time units (given by the inverse relaxation constants $t_0 \simeq 1/\Gamma \equiv 1$). At the end of this interval the dimensionless derivatives $\langle \partial \eta_1 / \partial t \rangle$ and $\langle \partial \eta_3 / \partial t \rangle$ go to values comparable with the intensity of the noise $\langle \xi_j(\mathbf{r},t) \rangle = 0$ and $\langle \xi_j(\mathbf{r},t) \xi_k(\mathbf{r}',t) \rangle = \delta_{jk} \delta(\mathbf{r}-\mathbf{r}') \delta(t-t')$.

This gives an estimation of the time sufficient to finish the ordering kinetics and reach a stationary state. One can prove that this time interval is sufficient at different values of the phenomenological parameters and the external field H. To compare, the time dependences of the averaged order parameter components $\langle \eta_1 \rangle$ and $\langle \eta_3 \rangle$ corresponding to the kinetic scenarios shown in Fig. 1 are presented in the inset to Figs. 3(a) and 3(b), respectively.

We use the above estimation for further calculations of the averaged stationary parameters as well as to plot physically the expected phase diagram. As was mentioned already, in spite of the qualitative differences between the two possible ordered states in the system, it can be characterized integrally by means of the averaged order parameter components $\langle \eta_1 \rangle$ and $\langle \eta_3 \rangle$. First let us calculate these values as functions from the external magnetic fields H at fixed values of the phenomenological constants. To do this, we start from the same initial conditions $\eta_1 \neq 0$ and $\eta_{2,3,4} = 0$ and repeat the above kinetic procedure during 2×10^3 time units at different values of H. The resulting field dependences of the components $\langle \eta_1 \rangle$ and $\langle \eta_3 \rangle$ at intermediate values of the constants $b_{2,3} = -0.2$ are shown in Fig. 4 as an example.

The same procedure can be repeated now for different constants from the physically interesting interval $-1.2 \leqslant b_{2,3} \leqslant 0.0$. It reproduces the corresponding dependences of the components $\langle \eta_1 \rangle$ and $\langle \eta_3 \rangle$ at any given external field H. In the inset to Fig. 4 we plot an example of such dependences at $H = 0.2$. It belongs to a region in the phase diagram where all changes of the parameters are quite pronounced.

Combining both types of dependences one can restore the phase diagram physically expected in the space $(b_{2,3};H)$. This diagram is presented in Fig. 5. Let us note once more that this phase diagram is a part of more complicated diagram. Generally speaking, it should be placed in at least a three-dimensional phase space $(b_2,b_3;H)$. One has to account for both signs of the constants $b_{2,3}$ also. It costs more computer time and this study is to be continued.

To summarize let us note that magnetic-field penetration to the superconductors with a multicomponent order parameter can cause new types of ordering. At some relation between parameters this ordered state can contain *two kinds of vortices* with a different (noninteger) value of the magnetic flux.

It should be noted once more that this deviation is caused by two reasons: the interaction between order parameter components and the interaction between vortices. Obviously, an isolated vortex carrying a noninteger flux quantum cannot exist. However, it does not mean directly, that these vortices always form pairs. In fact, we cannot observe an isolated pair. The structure found here is a collective effect and the vortices in the pair cannot be separated at distances larger than the London penetration depth, when their magnetic fluxes become really isolated. Strictly speaking, the statement about ''noninteger flux'' in this case means not more than that the structures of the order parameter and magnetic field in the vortex do not coincide with the structures for a ''standard'' isolated vortex in a traditional superconductor.

Numerical simulation of the process reproduces these new structures with two kinds of vortices at different internal parameters of the system. It gives a phase diagram of the system in a wide range of external magnetic field. Additional rearrangement of the structure due to an effective dipolar interaction lowers the symmetry of the vortex lattice down from an ordinary (hexagonal or tetragonal) one. This study can be applied to an experimental search for new structures in the ''heavy fermion'' superconductors,[6] in which multicomponent order parameters have been experimentally identified, in particular, in the well-known UPt_3 (see Ref. 7 and references therein).

The different vortices can be manifest in a specific correlation function for the magnetic-field density reproduced by the nontrivial positions and form factor of the peaks of SANS. The lattice of vortices as well as the absence of sixfold axes and general anisotropy of the peaks were observed by the SANS technique in different superconducting

compounds.[28–31] Unfortunately, a lot of the properties of the vortex lattice shadow the effects coming from anisotropic pairing in real experiments. A complicated variety of influences has to be excluded before resolution of the question about the role of unconventional pairing in the structure found from SANS measurements.[32]

ACKNOWLEDGMENTS

This work was supported in part by the CRDF foundation (Grant No. BP1-111) and the Fundamental Research Foundation of Ukraine (Project No. 2.4/199, Agreement No. F 72/97).

[1] G.E. Volovik and L.P. Gor'kov, Zh. Éksp. Teor. Fiz. **88**, 1412 (1985) [Sov. Phys. JETP **61**, 843 (1985)].
[2] M.E. Zhitomirsky, Zh. Éksp. Teor. Fiz. **97**, 1346 (1990) [Sov. Phys. JETP **70**, 760 (1990)].
[3] M. Heinila and G.E. Volovik, Physica B **210**, 330 (1995).
[4] T.Sh. Misirpashaev and G.E. Volovik, Physica B **210**, 338 (1995).
[5] Yu.M. Ivanchenko, A.A. Lisyansky, and A.E. Filippov, Fiz. Tverd. Tela (Leningrad) **31**, 51 (1989) [Sov. Phys. Solid State **31**, 51 (1989)].
[6] A.S. Zeltser, A.V. Radievsky, and A.E. Filippov, Zh. Éksp. Teor. Fiz. **112**, 1351 (1997) [Sov. Phys. JETP **85**, 734 (1997)].
[7] J.A. Sauls, Adv. Phys. **43**, 113 (1994).
[8] M.E. Zhitomirsky, J. Phys. Soc. Jpn. **64**, 913 (1995).
[9] J. Yeo and M.A. Moore, Phys. Rev. Lett. **78**, 4490 (1997).
[10] Q. Han and L. Zhang, Phys. Rev. B **56**, 11 942 (1997).
[11] Young Ren, Ji-Hai Xu, and C.S. Ting, Phys. Rev. Lett. **74**, 3680 (1995).
[12] U. Yaron, P.L. Gammel, G.S. Boebinger, G. Aeppli, P. Schiffer, E. Bucher, D.J. Bishop, C. Broholm, and K. Mortensen, Phys. Rev. Lett. **78**, 3185 (1997).
[13] R. Joynt, Phys. Rev. Lett. **78**, 3189 (1997).
[14] D.F. Agterberg, Phys. Rev. Lett. **80**, 5184 (1998).
[15] H. Won and K. Maki, Phys. Rev. B **53**, 5927 (1996).
[16] M. Ichioka, N. Hayashi, N. Enomoto, and K. Machida, Phys. Rev. B **53**, 15 316 (1996).
[17] M. Ichioka, A. Hasegawa, and K. Machida, Phys. Rev. B **59**, 8902 (1999).
[18] M. Franz, I. Affleck, and M.H.S. Amin, Phys. Rev. Lett. **79**, 1555 (1997).
[19] D. Chang, C.-Y. Mou, B. Rosenstein, and C.L. Wu, Phys. Rev. Lett. **80**, 145 (1998).
[20] Jian-Xin Zhu, Wonkee Kim, and C.S. Ting, Phys. Rev. B **58**, 15 020 (1998).
[21] C. Bolech, G.C. Buscaglia, and A. Lopez, Phys. Rev. B **52**, R15 719 (1995).
[22] R. Kato, Y. Enomoto, and S. Maekawa, Phys. Rev. B **47**, 8016 (1993).
[23] R. Kato, Y. Enomoto, and S. Maekawa, Phys. Rev. B **44**, 6916 (1991); M. Machida and H. Kaburaki, Phys. Rev. Lett. **71**, 3206 (1993).
[24] H. Frahm, S. Ullah, and A.T. Dorsey, Phys. Rev. Lett. **66**, 3067 (1991).
[25] S. Semenovskaya and A.G. Khachaturyan, Phys. Rev. Lett. **67**, 2223 (1991).
[26] Long-Qing Chen and A.G. Khachaturyan, Phys. Rev. B **46**, 5899 (1992).
[27] A.E. Filippov, Zh. Éksp. Teor. Fiz. **111**, 1775 (1997) [Sov. Phys. JETP **84**, 971 (1997)].
[28] J.W. Lynn, N. Rosov, T.E. Grigereit, H. Zhang, and T.W. Clinton, Phys. Rev. Lett. **72**, 3413 (1994).
[29] B. Keimer, W.Y. Shih, R.W. Erwin, J.W. Lynn, F. Dogan, and I.A. Aksay, Phys. Rev. Lett. **73**, 3459 (1994).
[30] B. Keimer, J.W. Lynn, R.W. Erwin, F. Dogan, W.Y. Shih, and I.A. Aksay, J. Appl. Phys. **76**, 6778 (1994).
[31] M. Yethiraj, D. McK. Paul, C.V. Tomy, and E.M. Forgan, Phys. Rev. Lett. **78**, 4849 (1997).
[32] S.T. Johnson, E.M. Forgan, S.H. Lloyd, C.M. Aegerter, S.L. Lee, R. Cubitt, P.G. Kealey, C. Ager, S. Tajima, A. Rykov, and D. McK. Paul, Phys. Rev. Lett. **82**, 2792 (1999).
[33] Y. Enomoto, R. Kato, K. Katsumi, and S. Maekawa, Physica C **192**, 166 (1992); **227**, 387 (1994).
[34] A.E. Filippov, A.V. Radievsky, and A.S. Zeltser, Phys. Rev. B **54**, 3504 (1996).
[35] Here and below the averaging in the $\langle \eta_j \rangle$ as well as in the $\langle \partial \eta_j / \partial t \rangle$ is performed with an absolute value of the corresponding order parameter component η_j. So it does not equal zero in the vortex state.
[36] D. Wei and G.N. Patey, Phys. Rev. Lett. **68**, 2043 (1992).
[37] J.J. Weis and D. Levesque, Phys. Rev. Lett. **71**, 2729 (1993).
[38] J. Ayton, M.I.P. Gingras, and G.N. Patey, Phys. Rev. Lett. **75**, 2360 (1995).
[39] I.M. Svishchev and P.G. Kusalik, Phys. Rev. Lett. **73**, 975 (1994); **75**, 3289 (1995).
[40] A.E. Filippov, Zh. Éksp. Teor. Fiz. **112**, 1739 (1997) [Sov. Phys. JETP **85**, 949 (1997)].
[41] A.K. Geim, I.V. Grigorieva, S.V. Dubonos, J.G.S. Lok, J.C. Maan, A.E. Filippov, and F.M. Peeters, Nature (London) **390**, 259 (1997).